Chinese Journal of Integrative Medicine
Available online at link.springer.com/journal/11655
Journal homepage: www.cjim.cn/zxyjhen/zxyjhen/ch/index.aspx
E-mail: cjim_en@cjim.cn

Original Article

Treg Immunomodulation Contributes to the Anti-atherosclerotic Effects of Huxin Formula in ApoE$^{-/-}$ Mice*

OU Xiao-min[1,2], CAI Jing[1,2], HU Xiao-yue[1,2], ZENG Qiao-huang[2], LAN Tao-hua[2,3], and JIANG Wei[2,3]

ABSTRACT **Objective**: To explore the effects of Huxin formula (HXF) in curtailing atherosclerosis and its underlying mechanism. **Methods**: According to random number table method, 24 specific pathogen free male ApoE$^{-/-}$ mice were randomly divided into model group, HXF low-dose (HXF-L) group (8.4 g/kg daily), HXF high-dose (HXF-H) group (16.8 g/kg daily), and pravastatin (8 mg/kg daily) group in Experiment Ⅰ (n=6 per group). C57BL/6J mice served as the control group (n=6). ApoE$^{-/-}$ mice in HXF-L, HXF-H, pravastatin groups were fed a Western diet and administered continuously by gavage for 12 weeks, while C57BL/6J mice in the control group were fed conventional lab mouse chow for 12 weeks. Further, Tregs were depleted by weekly intraperitoneal injection of purified anti-mouse CD25 antibody (PC61, 250 μg per mouse) for 4 weeks in Experiment Ⅱ (n=6 per group). Oil Red O and Masson staining were used to evaluate the plaque area and aortic root fibrosis. The CD4$^+$CD25$^+$Foxp3$^+$Treg counts in the lymph nodes and spleen cells were detected using flow cytometric analysis. The transforming growth factor-β1 (TGF-β1), interleukin (IL)-10, and IL-6 serum levels were examined by MILLIPLEX® MAP technology. Quantitative real-time reverse transcription PCR (qRT-PCR) and Western blot were utilized to assess the expression of TGF-β mRNA and protein in the aorta. The expression of CD4$^+$T lymphocytes, macrophages and smooth muscle cells in the aortic root were detected by immunofluorescence staining. **Results**: HXF reduced plaque area in ApoE$^{-/-}$ mice (P<0.01). HXF increased the Treg counts in the lymph nodes and spleen cells (P<0.05 or P<0.01). Moreover, HXF alleviated inflammatory response via elevating IL-10 and TGF-β1 serum levels (P<0.05), while decreasing the IL-6 serum levels in ApoE$^{-/-}$ mice (P>0.05). Also, HXF upregulated the expression of TGF-β mRNA and protein in the aorta (P<0.05). Additionally, HXF attenuated CD4$^+$T lymphocytes, macrophages and smooth muscle cells in aortic root plaque (P<0.01). Furthermore, the depletion of Tregs with CD25 antibody (PC61) curtailed the reduction in plaque area and aortic root fibrosis by HXF (P<0.01). **Conclusion**: HXF relieved atherosclerosis, probably by restraining inflammatory response, reducing inflammatory cell infiltration and attenuating aortic root fibrosis by increasing Treg counts.

KEYWORDS atherosclerosis, Huxin Formula, Tregs, immune responses, inflammation

Atherosclerosis is a major risk factor for various high-mortality cardiovascular and cerebrovascular diseases, such as myocardial infarction, stroke, gangrene and sudden death.[1] The pathogenesis of atherosclerosis involves lipid-driven endothelial dysfunction, inflammatory cell infiltration, smooth muscle cell migration, platelet aggregation, and fibrous plaque formation. In terms of clinical treatment, although Western drugs (such as statins and antithrombotic drugs) and percutaneous coronary intervention (PCI) can improve atherosclerosis patients' conditions, there is still room for improvement in their efficacy.[2] Globally, atherosclerosis continues to be the primary cause of morbidity and mortality, and it remains a challenge in the medical field that needs to be urgently tackled.

Atherosclerosis is widely considered a chronic inflammatory disease that is activated by innate and acquired immune responses.[3-5] Dendritic cells, macrophages, and T lymphocytes are among the

*Supported by the National Natural Science Foundation of China (No. 81874432) and Traditional Chinese Medicine Bureau of Guangdong Province (No. 20221172)
1. The Second Clinical College of Guangzhou University of Chinese Medicine, Guangzhou (510405), China; 2. Department of Cardiology, Guangdong Provincial Hospital of Chinese Medicine, the Second Affiliated Hospital of Guangzhou University of Chinese Medicine, Guangzhou (510020), China; 3. Guangdong Provincial Key Laboratory of Chinese Medicine for Prevention and Treatment of Refractory Chronic Diseases, Guangzhou (510020), China
Correspondence to: Dr. JIANG Wei, E-mail: jiangwei@gzucm.edu.cn
DOI: https://doi.org/10.1007/s11655-024-3663-2

immune cells that aggregate in atherosclerotic plaque, increasing inflammation.[6] Moreover, $CD4^+$T cells play a key role in atherosclerosis.[7] $CD4^+CD25^+Foxp3^+$ regulatory T cells (Tregs) are a subset of $CD4^+$T cells that maintains immune homeostasis by suppressing the function of effector T cells (Tcons). Tregs are characterized by the expression of forkhead/winged helix transcription factor (Foxp3). They release cytokines that reduce inflammation, such as transforming growth factor-β (TGF-β) and interleukin (IL)-10.[8] Extensive evidence has indicated that Treg cells have a protective effect against atherosclerosis.[7,9,10] Either a reduction in Treg counts or an impairment in immunosuppressive Treg function can facilitate atherosclerosis.[11,12] In contrast, *in vivo* treatment with IL-10-producing Tr1-like Tregs or pure spleen $CD4^+CD25^+$Tregs has been shown to decrease atherosclerosis in $ApoE^{-/-}$ mice, and produce a more permanent plaque phenotype.[13,14]

Huxin Formula (护心方, HXF) has the effects of benefiting qi, resolving phlegm, activating blood circulation and removing blood stasis, and has long been used to treat coronary heart disease (CHD). A previous study evaluated HXF's efficacy in patients with coronary artery disease (CAD) after revascularization in a multicenter, large-sample, randomized controlled clinical trial, and the results showed that HXF significantly improved CAD patients' quality of life.[15] In addition, HXF improved cardiac function grading in patients 1 year after surgery.[16] Meanwhile, an animal study has suggested that HXF reduces aortic atherosclerotic plaque formation in $ApoE^{-/-}$ mice.[17]

Although HXF has an exact efficacy in treating atherosclerosis and CAD, its underlying mechanism in atherosclerosis remains unclear. Since Chinese medicine (CM) is characterized by immune regulation and Tregs are key immunomodulatory cells that play a crucial role in preventing atherosclerosis, we speculated a possible connection between Tregs and HXF's anti-atherosclerotic effect. Thus, the purpose of this research was to investigate HXF's effect on atherosclerosis, and potential mechanisms based on Tregs.

METHODS

Drugs and Reagents

HXF composition are as follows: *Ginseng Radix et Rhizoma* (lot No. 210501) 10 g, *Citri Grandis Exocarpium* (lot No. 20210201) 6 g, *Notoginseng Radix et Rhizoma* (lot No. 210704041) 10 g, *Fructus Aurantii* (lot No. 210803041) 6 g, and *Carthami Flos* (lot No. 210804061) 10 g were acquired from Kangmei Pharmaceutical Co., Ltd., China. Pravastatin (Cat No. HY-B0165A) was purchased from MedChemExpress (China). Fluorescein isothiocyanate (FITC) CD4 monoclonal antibody (lot No. 2410094), PE-Cyanine7 CD25 monoclonal antibody (lot No. 2386301), APC Foxp3 monoclonal antibody (lot No. 2555811), and CD4 monoclonal antibody (GK1.5, lot No. 2297198) were acquired from eBioscience (USA). Foxp3/transcription factor fixation/permeabilization concentrate and diluent kit (Cat No. 00-5521-00) were purchased from eBioscience (USA). TGF-β1 single plex magnetic bead kit (Cat No. TGFBMAG-64K-01), anti-mouse IL-10 magnetic bead (Cat No. MIL10-MAG), and anti-mouse IL-6 magnetic bead (Cat No. MCYIL6-MAG) kit were purchased from Millipore (USA). Trizol reagent (lot No. 95141803) were manufactured from Invitrogen (USA). HiSoript Ⅲ RT SuperMix for qPCR (lot No. 7E691I2) and ChamQ Universal SYBR qPCR Master Mix (lot No. 7I642J2) were purchased from Vazyme Biotech Co., Ltd., China. Mouse-TGF-β primers (lot No. 2114186784 and 2114186785) and mouse-GAPDH primers (lot No. GA28KA7468) were purchased from Sangon Biotech (China). Primary antibodies TGF-β (Cat No. 3711), GAPDH (Cat No. 5174), CD68 (E3O7V) rabbit mAb (Cat No. 97778), α-smooth muscle actin (α-SMA, D4K9N) XP® Rabbit mAb (Cat No. 19245), and secondary antibody horseradish peroxidase (HRP) anti-rabbit IgG (Cat No. 7074), Alexa Fluor® 594 Conjugate anti-rabbit IgG (Cat No. 8889), and Alexa Fluor® 647 Conjugate anti-rat IgG (Cat. No. 4418) were acquired from Cell Signaling Technology (USA). Ultra-LEAF™ Purified anti-mouse CD25 antibody (Cat No. 102059) were obtaied from Biolegend (USA).

Preparation of HXF Decoction

All compositions of HXF were mixed and soaked in water for 30 min (the ratio of water to HXF composition was 8 mL:1 g), and then decocted for 30 min for the first time. The decoction was filtered through 4 layers of gauze and then collected. The second decoction was boiled with water (the ratio of water to HXF compositions was 6 mL:1 g) for 30 min. The decoctions were combined and rotary evaporated to concentrations of 0.42 g/mL and 0.84 g/mL (low concentration and high concentration, respectively). The dosage was converted according to the body

surface area of human and mouse. The methods and results of the fingerprint analysis of the active ingredients of HXF are provided in Appendix 1.

Animals and Drug Administration

Eight-week-old C57BL/6J mice and ApoE$^{-/-}$ mice (specific pathogen free grade, male, 18–22 g) were purchased from Guangdong Medical Laboratory Animal Center (Guangzhou, China). All mice were housed in a specific pathogen-free room maintained at 23 ℃ and 65% humidity, under a 12-h light/dark cycle, with free access to food and water. All experiments were approved by the Institutional Animal Ethical Committee at the Guangdong Provincial Academy of Chinese Medical Sciences (No. 2019021).

According to random number table method, 24 ApoE$^{-/-}$ mice were randomly divided into the model group, HXF low-dose (HXF-L) group, HXF high-dose (HXF-H) group, and pravastatin group in Experiment Ⅰ (n=6 per group). C57BL/6J mice served as the control group (n=6). HXF low-dose (8.4 g/kg daily, 0.42 g/mL HXF decoction, 0.2 mL/10 g of body weight) and high-dose (16.8 g/kg daily, 0.84 g/mL HXF decoction, 0.2 mL/10 g of body weight) were intragastrically administered to ApoE$^{-/-}$ mice in the HXF-L and the HXF-H groups respectively for 12 weeks. Pravastatin was dissolved in 0.5% sodium carboxymethyl cellulose. It was then intragastrically administered to the ApoE$^{-/-}$ mice in the pravastatin group (8 mg/kg daily) for 12 weeks.

In Experiment Ⅱ, Treg depletion was conducted using purified anti-mouse CD25 antibody (PC61) to determine if it could inhibit the anti-atherosclerotic effect of HXF-H. Twenty-four ApoE$^{-/-}$ mice were randomized into the model group, HXF-H group, pravastatin group, and CD25 antibody+HXF-H group (n=6 per group). C57BL/6J mice are the control group (n=6). The mice in the CD25 antibody+HXF-H group were given HXF-H intragastrically for 12 weeks, and then were intraperitoneally injected with CD25 antibody (250 μg per mouse) weekly for 4 weeks. All ApoE$^{-/-}$ mice received *ad libitum* access to a Western diet (21% fat, 1.5% cholesterol), while the C57BL/6J mice were fed conventional lab mouse chow for 12 weeks.

Sample Collection

Following the experiment, the mice were anesthetized with 0.5% sodium pentobarbital solution and their eyeballs were removed to collect blood. The blood samples were centrifuged at 3,500 r/min, 4 ℃ for 15 min, and the serum was extracted for the detection of inflammatory cytokines. The aortic root, which is connected to the heart, was extracted for Oil Red O staining, Masson staining, and immunofluorescence staining. Full-length aortas were isolated for quantitative real-time reverse transcription PCR (qRT-PCR) and Western blot analysis. Additionally, the spleen and draining lymph nodes were removed to isolate cells for flow cytometry analysis.

Cytokine Assay

The levels of TGF-β1, IL-10, and IL-6 in mouse serum were measured using the MILLIPLEX® MAP (MILLIPLEX® MAGPI, Luminex, USA), which is based on Luminex® xMAP® technology and carried out according to the manufacturer's instructions.

Flow Cytometric Analysis

Cells from spleen and lymph node were collected and incubated with CD4 and CD25 monoclonal antibodies at room temperature, and protected from light for 30 min. Then, the cells were incubated by Foxp3/transcription factor fixation/permeabilization concentrate and a diluent kit at room temperature, and protected from light for at least 30 min. The cells were further incubated with APC Foxp3 monoclonal antibody protected from light for about 30 min. Ultimately, the cells underwent washing and were examined with a flow cytometer (Novo Quanteon, USA).

Oil Red O Staining

The hearts containing the aortic root were placed in an optimal cutting temperature (OCT) compound and subsequently frozen at a temperature of –80 ℃. Cryosections were performed on the hearts containing the aortic root specimens, followed by staining with Oil Red O to identify and analyze any atherosclerotic lesions. The plaque area and lipid deposition area percentages were quantified with Image J (National Institutes of Health, USA).

Masson Staining

Any hearts containing the aortic root were isolated, fixed for at least 24 h in 4% paraformaldehyde, dehydrated, and paraffin-embedded. Masson staining was performed according to the manufacturer's protocols for the Masson staining kit. A light microscope was used to examine the stained slices.

Immunofluorescence Staining

The expression of CD4 ($CD4^+$T lymphocytes), CD68 (macrophages) and α-SMA (smooth muscle cells) in aortic root plaque were detected by immunofluorescence staining. Frozen slices of aortic root were incubated with the primary antibodies anti-CD4, anti-CD68, anti-α-SMA, overnight at 4 ℃, then stained using a secondary antibody. Then, 4',6-diamidino-2-phenylindole (DAPI) was applied to the frozen slices. Image J was employed to analyze the stained sections after they were viewed under a fluorescence microscope.

qRT-PCR

Total RNA from full-length aortas was extracted with Trizol reagent. The process of transcribing mRNA into cDNA was conducted using a HiSoript Ⅲ RT SuperMix kit, according to the manufacturer's instructions. The primer sequences were: TGF-β, forward, 5'-ACCGCAACAACGCCATCTATGAG-3', and reverse, 5'- GGCACTGCTTCCCGAATGTCTG-3'; GAPDH, forward, 5'- GGTTGTCTCCTGCGACTTCA-3', and reverse, 5'- TGGTCCAGGGTTTCTTACTCC-3'. The ChamQ Universal SYBR qPCR Master Mix was used in the qRT-PCR reaction performed with the CFX Manager 2.1 system (Bio-Rad, USA). Every sample underwent triplicate analysis, with each analysis standardized to GAPDH. The analysis was performed using a $2^{-\triangle\triangle Ct}$ method.

Western Blot

Protein samples were extracted from full-length aortas using radioimmunoprecipitation assay (RIPA) buffer, and the protein quantities were measured using a bicinchoninic acid (BCA) protein assay kit. An equal quantity of proteins (40 μg) was subjected to separation using 12% sodium dodecyl sulfate-polyacrylamide gel electrophoresis (SDS-PAGE) gelelectrophoresis, and thereafter moved on to the polyvinylidene difluoride (PVDF) membrane. Then the PVDF membranes were blocked with 5% skim milk for 1 h, and incubated with primary antibody TGF-β (1:1,000) and GAPDH (1:10,000) overnight at 4 ℃. Next, the membranes were washed 3 times, and then the membranes were incubated for 1 h with secondary antibody HRP anti-rabbit IgG. Blot detection was accomplished using Bio-Rad Image Lab software and employing the chemiluminescence (ECL) technique. The band intensities were measured using Image Lab.

Statistical Analysis

All data were presented as mean ± standard deviation ($\bar{x} \pm s$) and analyzed with SPSS 26.0 software (IBM Statistics, USA). One-way analysis of variance (ANOVA) was utilized to conduct statistical analysis on various groups. The least significant difference (LSD) test was applied when homogeneity of variances was assumed, while Dunnett's T3 test was used when homogeneity of variances was not assumed. A value of $P<0.05$ was considered statistically significant.

RESULTS

HXF Reduced Plaque Area in Aortic Roots of $ApoE^{-/-}$ Mice

As shown in Figure 1, no atherosclerotic lesions were observed in the control mice, while the model mice fed with a Western diet had developed obvious atherosclerotic plaque ($P<0.05$). In contrast to the model group, the mice who received HXF-L, HXF-H, or pravastatin treatment exhibited a reduction in lipid deposition and plaque area, the effect of HXF-H was more obvious ($P<0.01$).

HXF Induced $CD4^+CD25^+Foxp3^+$Tregs in Lymph Nodes and Spleen Cells

As represented in Figure 2, the Treg quantities of lymph nodes in the model group decreased, compared with the control group ($P<0.01$). HXF-L, HXF-H or pravastatin treatment augmented the Treg counts as compared to the model group ($P<0.01$). Moreover, HXF-H increased the Treg counts more drastically than HXF-L and pravastatin. In addition, splenic Tregs and lymph node Tregs showed a similar trend. Compared with the control group, splenic Tregs decreased in

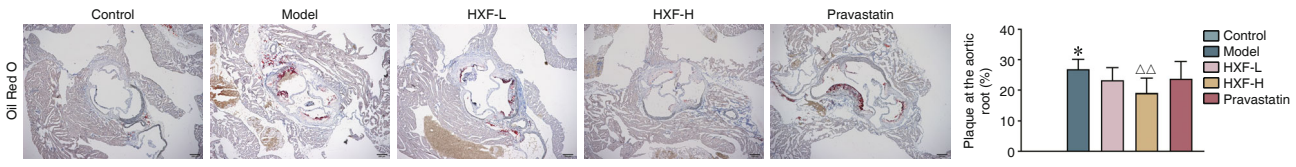

Figure 1. HXF Reduced Plaque Area in the Aortic Root ($\bar{x} \pm s$, n=6)

Notes: Representative images of Oil Red O (×40 magnification), scale bar=200 μm; $^*P<0.01$ *vs*. control group, $^\triangle P<0.05$ *vs*. model group

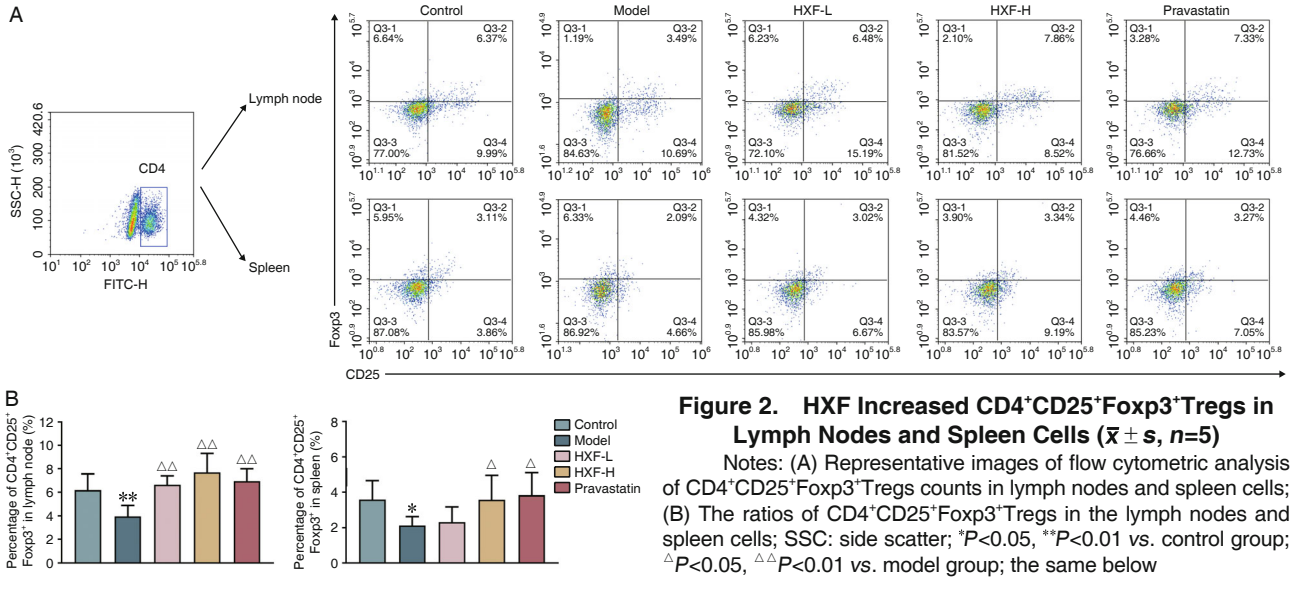

Figure 2. HXF Increased CD4⁺CD25⁺Foxp3⁺Tregs in Lymph Nodes and Spleen Cells ($\bar{x} \pm s$, n=5)

Notes: (A) Representative images of flow cytometric analysis of CD4⁺CD25⁺Foxp3⁺Tregs counts in lymph nodes and spleen cells; (B) The ratios of CD4⁺CD25⁺Foxp3⁺Tregs in the lymph nodes and spleen cells; SSC: side scatter; $^{*}P$<0.05, $^{**}P$<0.01 *vs*. control group; $^{\triangle}P$<0.05, $^{\triangle\triangle}P$<0.01 *vs*. model group; the same below

the model group (P<0.05). Additionally, HXF-H and pravastatin significantly augmented splenic Tregs compared with the model group (P<0.05). The HXF-L group showed a slight increase in splenic Tregs, but it was not statistically significant (P>0.05).

HXF Increased Serum Levels of IL-10 and TGF-β 1, and Decreased Serum IL-6

As shown in Figure 3, the IL-10 and TGF-β 1 serum levels in the model group were lower than those in the control group (P<0.05 or P<0.01). Additionally, HXF-H administration showed an increase in the IL-10 and TGF-β 1 serum concentrations when compared to the model group (P<0.05). Both HXF-L and pravastatin treatments showed a trend of increasing IL-10 levels, with HXF-L also demonstrating a slight elevation in TGF-β 1 levels. In contrast, the model group exhibited higher IL-6 serum levels compared with the control group, while IL-6 levels decreased in the HXF-L and HXF-H groups compared with the model group, with no statistical difference (P>0.05).

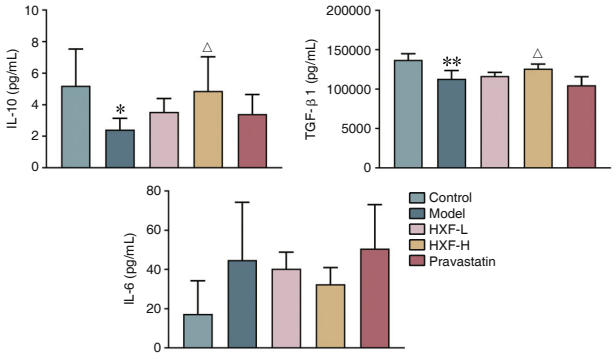

Figure 3. HXF Increased Serum IL-10 and TGF-β 1 Levels and Decreased IL-6 Levels ($\bar{x} \pm s$, n=5)

HXF Increased TGF-β mRNA and Protein Expressions in Aortas of ApoE$^{-/-}$ Mice

As presented in Figure 4, the model group manifested a slight decrease in the TGF-β mRNA and protein expressions relative to the control group (P>0.05). The administration of HXF-H resulted in a considerable increase in TGF-β mRNA expression (P<0.01), and showed a tendency toward upregulating TGF-β protein expression (P>0.05), compared with the model group.

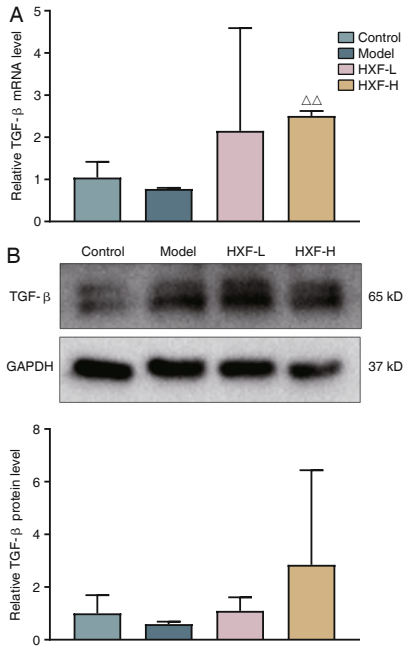

Figure 4. HXF Upregulated TGF-β mRNA and Protein Expression Levels ($\bar{x} \pm s$, n=3)

Notes: (A) The relative mRNA level of the TGF-β in the aortas was tested by qPCR; (B) The protein expression of TGF-β in the aortas was measured by Western blot

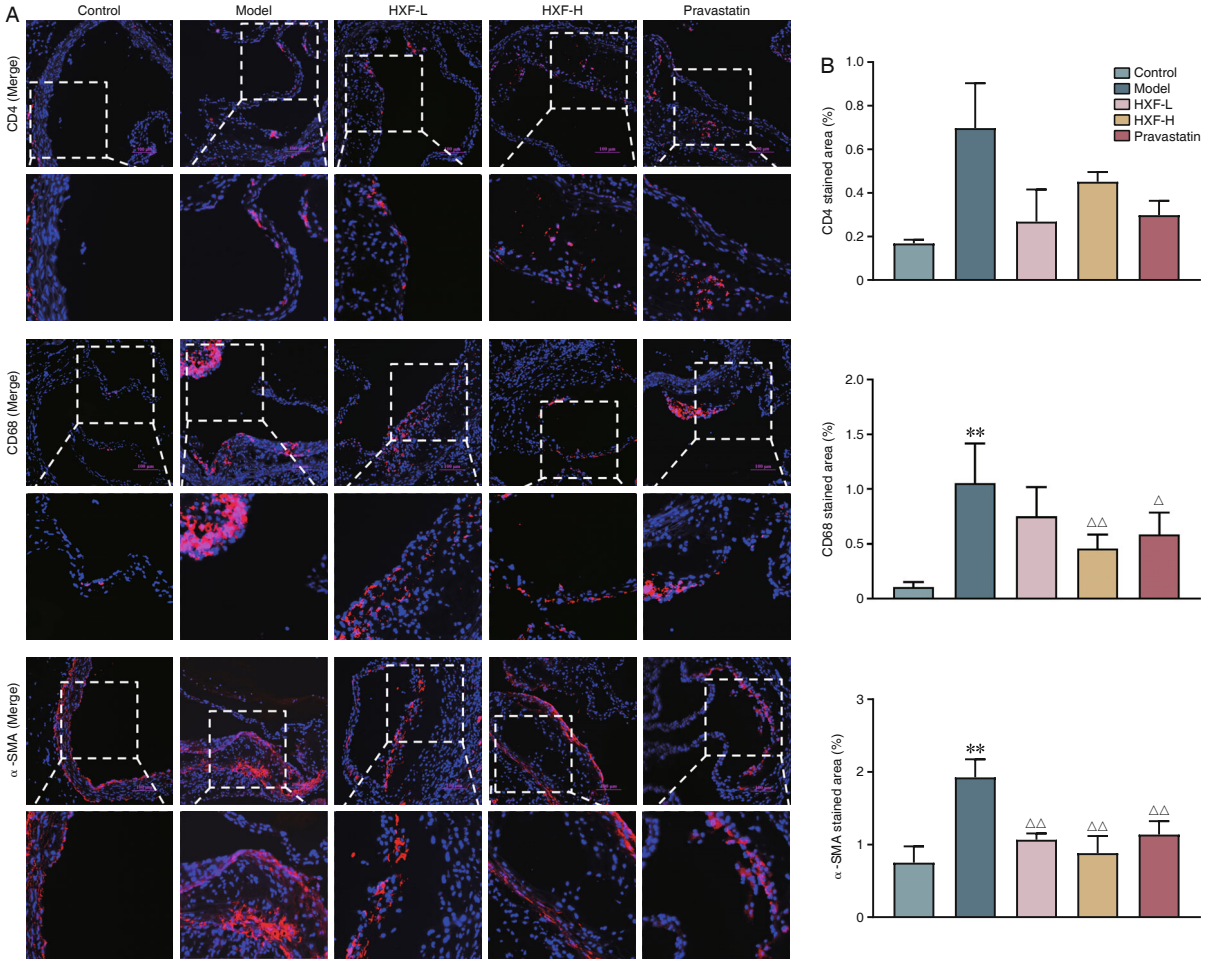

Figure 5. HXF Suppressed Infiltration of CD4⁺T cells, Macrophages and Smooth Muscle Cells in Atherosclerotic Plaque of ApoE$^{-/-}$ Mice ($\bar{x} \pm s$)

Notes: (A) Representative images of immunofluorescence of CD4 (representing CD4⁺T cells), CD68 (representing macrophages), and α-SMA (representing smooth muscle cells), scale bar=100 μm; (B) The CD4 (n=3), CD68 and α-SMA (n=4) stained area percentages

HXF Inhibited Infiltration of CD4⁺T Cells, Macrophages and Smooth Muscle Cells in Aortic Root Plaque of ApoE$^{-/-}$ Mice

Immunofluorescence analysis revealed that in comparison with the control group, the model group showed an increasing trend in CD4 positive area (CD4⁺T cells), with a significant increase in CD68 (macrophages) and α-SMA (smooth muscle cells) positive areas (P<0.01). Compared with the model group, the CD4 positive area in the HXF-L, HXF-H, and pravastatin groups exhibited a decreasing trend, with a significant decrease in CD68 and α-SMA positive areas (P<0.01 or P<0.05, Figure 5).

CD25⁺ Treg Depletion Blocked Reduction in Plaque Area and Aortic Root Fibrosis by HXF

As presented in Figures 6A and 6B, Western diet-fed ApoE$^{-/-}$ mice in the model group had obvious plaque formation, with large amounts of lipid deposition in the aortic roots (P<0.05). No significant atherosclerotic plaque was found in the control group. Compared with the model group, the plaque area decreased in the HXF-H and pravastatin groups (P<0.01 or P<0.05). Masson staining consistently exhibited that the collagen fiber content in the model group was much higher than that in the control group. Additionally, HXF-H and pravastatin treatment decreased collagen deposition. Furthermore, CD25⁺Treg depletion inhibited the alleviation of plaque area (P<0.01) and fibrosis by HXF-H.

As depicted in Figures 6C–6E, the model mice presented a reduction in the Treg counts in the lymph nodes, in comparison to the control mice (P<0.01). In comparison to the model group, the Treg counts in the lymph nodes significantly increased in the HXF-H and pravastatin groups (P<0.01). In contrast, splenic Tregs were downregulated in the model group compared

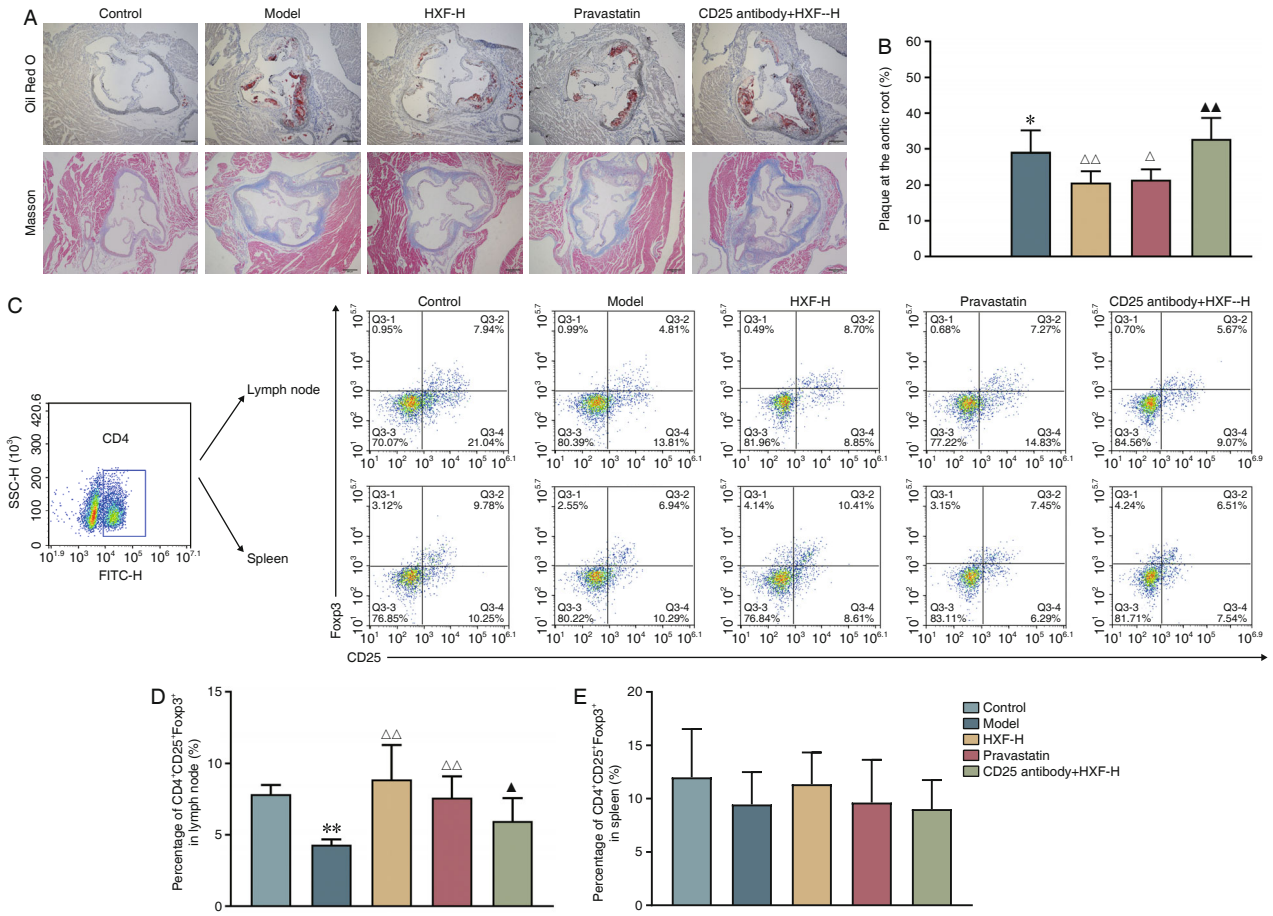

Figure 6. CD25⁺ Treg Depletion Blocked Effect of HXF on Reducing Plaque Area and Aortic Root Fibrosis ($\bar{x} \pm s$)

Notes: (A) Representative images of Oil Red O and Masson staining (×40 magnification), scale bar=200 μm; (B) The ratios of plaque area in the aortic root (n=6); (C) Representative images of flow cytometric analysis of $CD4^+CD25^+Foxp3^+$Tregs counts in lymph nodes and spleen cells; (D and E) The ratios of $CD4^+CD25^+Foxp3^+$Tregs in the lymph nodes (n=4) and spleen cells (n=5); $^*P<0.01$ *vs*. control group; $^{\triangle\triangle}P<0.01$ *vs*. model group; $^{\blacktriangle}P<0.05$, $^{\blacktriangle\blacktriangle}P<0.01$ *vs*. HXF group

with the control group, while they were upregulated in the HXF-H and pravastatin groups. Furthermore, upregulation effect of HXF-H was more prominent. However, no statistical difference was observed (P>0.05). Additionally, CD25 antibodies depleted the increase in Tregs by HXF-H in the lymph nodes cells (P<0.05).

DISCUSSION

Cardiovascular disease accounts for one-third of all deaths worldwide, and atherosclerosis is a major cause of it. Atherosclerosis is a complex disease that progresses slowly and continues to affect individuals throughout their lives. However, a complete understanding of the etiology of atherosclerosis remains elusive. Therefore, there is an urgent need to clarify its mechanism and explore more effective and safer therapeutic strategies. Over the last decade, immune regulation's role in atherosclerosis has attracted much attention. Many studies have reported that Tregs have a protective role in atherosclerosis prevention.[18-20] CM has the advantage of regulating immune function with few side effects, yet there have been few studies on treatment of atherosclerosis with CM. Scientific evidence has shown that HXF is effective in patients with CHD, and reduces the development of atherosclerotic plaque in mice.[15-17] This study was designed to evaluate potential protective of HXF on atherosclerosis through the regulation of Tregs, from an immunological perspective.

$ApoE^{-/-}$ mice are a widely employed animal model for studying atherosclerosis. In the present investigation, we utilized a Western diet to induce the occurrence of atherosclerosis in $ApoE^{-/-}$ mice, as indicated by the notable increase in plaque at the aortic root in the model group. HXF-L, HXF-H and pravastatin administration reduced the plaque area

in the aortic root, and HXF-H produced even better results. Extensive animal experimental data have demonstrated Tregs' protective role in atherosclerosis. A study showed that surgical stress response resulted in a notable rise in atherosclerotic plaque necrosis in mice treated with CD25 antibodies, while the injection of IL-2/anti-IL-2 complex (IL-2C), which promoted Tregs amplification, notably improved postoperative atherosclerotic plaque stability.[21] Moreover, Zhu, et al[22] developed a fusion protein with greater IL-2Rα affinity than IL-2. In an ApoE$^{-/-}$ mouse model, this IL-2 fusion protein hindered atherosclerosis advancement by stimulating and enhancing Treg. In contrast, depletion of Foxp3^{+} Tregs by diphtheria toxin injection enhances CD4^{+} effector T-cell immunoreactivity and exacerbates atherosclerosis.[23] Clinical trials have also demonstrated Tregs' role in human atherosclerosis.[24-26] In our study, flow cytometric analysis showed that the CD4^{+}CD25^{+}Foxp3^{+}Treg counts in lymph nodes and spleen had decreased in the model group. Of note, the Treg counts in the spleen and lymph nodes cells manifested an increasing effect for the HXF and pravastatin groups, with the HXF-H group having the best effect. Thus, our data indicated that HXF's anti-atherosclerosis effect might be related to Tregs.

Atherosclerosis is an immune-activated chronic inflammatory disease. Two recent clinical trials have shown that anti-inflammatory therapies have a beneficial effect on atherosclerosis.[27,28] It has also been confirmed that IL-10 and TGF-β, two Treg-mediated anti-inflammatory factors, have strong anti-atherosclerotic effects.[8,29,30] Additionally, macrophage-produced IL-6 promotes vascular inflammation and aggravates of atherosclerosis.[31] Our research showed that the model group had reduced serum concentrations of IL-10 and TGF-β1, while presenting elevated IL-6 levels compared to the control group. Moreover, HXF-H treatment contributed to an increase in the IL-10 and TGF-β1 concentrations, while demonstrating a potential negative effect on IL-6 levels when compared to the model group. On the other hand, TGF mRNA and protein expressions decreased slightly in the aortas of the model group, whereas HXF-H significantly increased TGF mRNA and protein levels. These data demonstrated that the inflammatory response had been relieved following intervention with HXF-H.

CD4^{+}T cells, macrophages, and smooth muscle cells are vital components of atherosclerotic plaques. In the presence of chemokines, CD4^{+}T cells and macrophages collect in atherosclerotic plaques, releasing pro-inflammatory factors and promoting the development of atherosclerosis.[32,33] Meanwhile, macrophages ingest large amounts of lipids, which are converted into foam cells, and aggravate atherosclerosis.[34,35] The migration and proliferation of smooth muscle cells play a significant role in establishing neointima and in atherosclerotic plaque development.[36] In this study, immunofluorescence analysis showed that HXF and pravastatin administration inhibit the infiltration of macrophages and smooth muscle cells in atherosclerotic plaque, and the inhibitory effect of HXF-H is even more obvious. Moreover, treatment with HXF and pravastatin have a tendency to repress CD4^{+}T cell infiltration. These findings revealed that HXF suppresses inflammatory cell invasion in atherosclerotic plaque.

To further confirm Tregs' role in HXF's anti-atherosclerosis effect, Western diet-fed ApoE$^{-/-}$ mice were treated with HXF-H, and then were depleted of CD25^{+}Tregs by CD25 antibody. Oil Red O analysis showed that the aortic roots exhibited substantial plaque generation in the model group, whereas the plaque was significantly smaller in the HXF-H and pravastatin groups. Fibrosis is a compensatory process of tissue damage caused by chronic inflammation, and it is an important factor behind atherogenesis. The proliferation of fibrous tissue allows fatty streaks in atherosclerosis to evolve into pathologic fibrous plaques, narrowing the lumen and impeding blood flow. The rupture of unstable fibrous plaque can lead to thrombosis and stroke risk events.[37] This research has shown a large buildup of collagen fibers in the aortic root plaque in the model group. The mice receiving HXF-H and pravastatin had a reduction in fibrosis, with the most marked drop observed in the HXF-H treated group. Furthermore, the depletion of Tregs with CD25 antibodies significantly curtailed the reduction in atherosclerotic plaque area and fibrosis by HXF-H treatment. Additionally, flow cytometry data verified again that Tregs had decreased in the model group and elevated in the HXF-H and pravastatin groups. Moreover, CD25 antibody mitigated the increase in Tregs by HXF-H. These findings suggest that Tregs are involved in the underlying mechanism of HXF-attenuating atherosclerosis.

In conclusion, our study has shown that HXF

attenuated atherosclerosis progression, possibly by resisting inflammatory response, reducing inflammatory cell infiltration and decreasing the extent of fibrosis in atherosclerotic plaque by elevating Tregs. This provides new ideas for therapeutic atherosclerosis strategies, and provides a laboratory basis for the clinical application of HXF. However, the upstream pathways through which HXF regulates Tregs, and the balance between Tregs and other immune cells in atherosclerosis, remain unclear and warrant further exploration.

Conflict of Interest

All authors declare no conflicts of interest.

Author Contributions

Ou XM performed the experiments, analyzed the data and wrote the manuscript. Cai J performed the experiments and analyzed the data. Hu XY conducted the literature search and data collection. Zeng QH performed the experiments. Lan TH directed and revised the manuscript. Jiang W conceived and designed the experiments. All authors confirmed the final manuscript and approved it for publication.

Electronic Supplementary Material: Supplementary materials (Appendixes) are available in the online version of this article at https://doi.org/10.1007/s11655-024-3663-2.

REFERENCES

1. Bjorkegren JLM, Lusis AJ. Atherosclerosis: recent developments. Cell 2022;185:1630-1645.
2. Sharma M, Schlegel MP, Afonso MS, Brown EJ, Rahman K, Weinstock A, et al. Regulatory T cells license macrophage pro-resolving functions during atherosclerosis regression. Circ Res 2020;127:335-353.
3. Wolf D, Ley K. Immunity and inflammation in atherosclerosis. Circ Res 2019;124:315-327.
4. Ley K. Role of the adaptive immune system in atherosclerosis. Biochem Soc Trans 2020;48:2273-2281.
5. Roy P, Orecchioni M, Ley K. How the immune system shapes atherosclerosis: roles of innate and adaptive immunity. Nat Rev Immunol 2022;22:251-265.
6. Lecis D, Massaro G, Benedetto D, Di Luozzo M, Russo G, Mauriello A, et al. Immunomodulation therapies for atherosclerosis: the past, the present, and the future. Int J Mol Sci 2023;24:10979.
7. Saigusa R, Winkels H, Ley K. T cell subsets and functions in atherosclerosis. Nat Rev Cardiol 2020;17:387-401.
8. Wang Q, Wang YR, Xu DY. Research progress on Th17 and T regulatory cells and their cytokines in regulating atherosclerosis. Front Cardiovasc Med 2022;9:929078.
9. Ait-Oufella H, Lavillegrand JR, Tedgui A. Regulatory T cell-enhancing therapies to treat atherosclerosis. Cells 2021;10:723.
10. Ali AJ, Makings J, Ley K. Regulatory T cell stability and plasticity in atherosclerosis. Cells 2020;9:2665.
11. Klingenberg R, Gerdes N, Badeau RM, Gistera A, Strodthoff D, Ketelhuth DF, et al. Depletion of Foxp3^{+} regulatory T cells promotes hypercholesterolemia and atherosclerosis. J Clin Invest 2013;123:1323-1334.
12. Spitz C, Winkels H, Burger C, Weber C, Lutgens E, Hansson GK, et al. Regulatory T cells in atherosclerosis: critical immune regulatory function and therapeutic potential. Cell Mol Life Sci 2016;73:901-922.
13. Mallat Z, Gojova A, Brun V, Esposito B, Fournier N, Cottrez F, et al. Induction of a regulatory T cell type 1 response reduces the development of atherosclerosis in apolipoprotein e-knockout mice. Circulation 2003;108:1232-1237.
14. Feng J, Zhang Z, Kong W, Liu B, Xu Q, Wang X. Regulatory T cells ameliorate hyperhomocysteinaemia-accelerated atherosclerosis in ApoE$^{-/-}$ mice. Cardiovasc Res 2009;84:155-163.
15. Wu HL, Wang YF, Li JZ, Zhang MZ, Sheng XG, Wang X, et al. A multicentre randomized clinical trial on efficacy and safety of Huxin Formula in patients undergoing percutaneous coronary intervention. Evid Based Complement Alternat Med 2014;2014:143064.
16. Lin Y, Wang YF, Lin DQ, Chen JW, Li JZ, Lan TH, et al. Efficacy and safety of Huxin Formula in patients after CABG: a multicenter, double-blind, randomized clinical trial. Forsch Komplementmed 2014;21:351-359.
17. Jiang W, Li S, Mao W, Yang G, Li XM, Zheng GJ, et al. Effect of Huxin Formula on reverse cholesterol transport in apoe-gene knockout mice. Chin J Integr Med 2012;18:451-456.
18. Ou HX, Guo BB, Liu Q, Li YK, Yang Z, Feng WJ, et al. Regulatory T cells as a new therapeutic target for atherosclerosis. Acta Pharmacol Sin 2018;39:1249-1258.
19. Tanaka T, Sasaki N, Rikitake Y. Recent advances on the role and therapeutic potential of regulatory T cells in atherosclerosis. J Clin Med 2021;10:5907.
20. Wang XT, Zhou H, Liu Q, Cheng PP, Zhao TY, Yang TS, et al. Targeting regulatory T cells for cardiovascular diseases. Front Immunol 2023;14:1126761.
21. Handke J, Kummer L, Weigand MA, Larmann J. Modulation of peripheral CD4^{+}CD25^{+}Foxp3^{+} regulatory T cells ameliorates surgical stress-induced atherosclerotic plaque progression in apoe-deficient mice. Front Cardiovasc Med 2021;8:682458.
22. Zhu XY, Li QZ, George V, Spanoudis C, Gilkes C, Shrestha N, et al. A novel interleukin-2-based fusion molecule, HCW9302,

differentially promotes regulatory T cell expansion to treat atherosclerosis in mice. Front Immunol 2023;14:1114802.
23. Kasahara K, Sasaki N, Amin HZ, Tanaka T, Horibe S, Yamashita T, et al. Depletion of Foxp3$^+$ regulatory T cells augments CD4$^+$ T cell immune responses in atherosclerosis-prone hypercholesterolemic mice. Heliyon 2022;8:e09981.
24. Joly AL, Seitz C, Liu S, Kuznetsov NV, Gertow K, Westerberg LS, et al. Alternative splicing of Foxp3 controls regulatory T cell effector functions and is associated with human atherosclerotic plaque stability. Circ Res 2018;122:1385-1394.
25. Klingenberg R, Brokopp CE, Grives A, Courtier A, Jaguszewski M, Pasqual N, et al. Clonal restriction and predominance of regulatory T cells in coronary thrombi of patients with acute coronary syndromes. Eur Heart J 2015;36:1041-1048.
26. Potekhina AV, Pylaeva E, Provatorov S, Ruleva N, Masenko V, Noeva E, et al. Treg/Th17 balance in stable cad patients with different stages of coronary atherosclerosis. Atherosclerosis 2015;238:17-21.
27. Ridker PM, Everett BM, Thuren T, MacFadyen JG, Chang WH, Ballantyne C, et al. Antiinflammatory therapy with canakinumab for atherosclerotic disease. N Engl J Med 2017;377:1119-1131.
28. Tardif JC, Kouz S, Waters DD, Bertrand OF, Diaz R, Maggioni AP, et al. Efficacy and safety of low-dose colchicine after myocardial infarction. N Engl J Med 2019;381:2497-2505.
29. Baardman J, Lutgens E. Regulatory T cell metabolism in atherosclerosis. Metabolites 2020;10:279.
30. Hu WL, Li JY, Cheng X. Regulatory T cells and cardiovascular diseases. Chinese Med J 2023;136:2812-2823.
31. Garshick MS, Ward NL, Krueger JG, Berger JS. Cardiovascular risk in patients with psoriasis: JACC review topic of the week. J Am Coll Cardiol 2021;77:1670-1680.
32. Forrester SJ, Kikuchi DS, Hernandes MS, Xu Q, Griendling KK. Reactive oxygen species in metabolic and inflammatory signaling. Circ Res 2018;122:877-902.
33. Tousoulis D, Oikonomou E, Economou EK, Crea F, Kaski JC. Inflammatory cytokines in atherosclerosis: current therapeutic approaches. Eur Heart J 2016;37:1723-1732.
34. Maguire EM, Pearce SWA, Xiao Q. Foam cell formation: a new target for fighting atherosclerosis and cardiovascular disease. Vascul Pharmacol 2019;112:54-71.
35. Ford HZ, Byrne HM, Myerscough MR. A lipid-structured model for macrophage populations in atherosclerotic plaques. J Theor Biol 2019;479:48-63.
36. Grootaert MOJ, Bennett MR. Vascular smooth muscle cells in atherosclerosis: time for a re-assessment. Cardiovasc Res 2021;117:2326-2339.
37. Singh S, Torzewski M. Fibroblasts and their pathological functions in the fibrosis of aortic valve sclerosis and atherosclerosis. Biomolecules 2019;9:472.

(Accepted February 21, 2024)
Edited by ZHANG Wen